JOURNAL OF APPLIED ELECTROCHEMISTRY 17 (1987) 1129–1143

Characterization of impurity effects in zinc electrowinning from industrial acid sulphate electrolyte

D. J. MACKINNON, J. M. BRANNEN, P. L. FENN

Metallurgical Chemistry Section, Mineral Sciences Laboratories, CANMET, Energy, Mines and Resources Canada, 555 Booth Street, Ottawa, Ontario, Canada K1A 0G1

Received 18 February 1987

The individual effects of 15 impurities and their interaction with glue on zinc electrowinning from industrial acid sulphate electrolyte were characterized in terms of deposit morphology and preferred deposit orientation and in terms of current efficiency and zinc deposition polarization behaviour. The current efficiency decreased in a cyclical manner with increasing atomic number of the impurity element in each period of the periodic table. This decrease in current efficiency can be correlated to a corresponding increase in the rate of hydrogen evolution on the impurity metal. The various impurities produced four distinct zinc deposit morphologies and orientations and also produced characteristic changes in the cyclic voltammograms for the zinc deposition.

1. Introduction

The zinc electrowinning process is very sensitive to the presence of impurities in the electrolyte. Neutral purification eliminates the bulk of the impurities, but in certain instances their concentrations still may be high enough to cause difficulties in zinc electrowinning. Impurity behaviour is not well understood in spite of the many studies which document impurity effects on the current efficiency (CE), and the more recent work which characterizes impurity effects on zinc deposit morphology and orientation and on zinc deposition polarization.

The ease with which hydrogen ions can be reduced in solution in the presence of the impurity is a critical factor. The fact that certain impurities, e.g. Ge, Sb, are hydride formers may facilitate the reduction of hydrogen ions for these impurities. Other impurities such as Ni and Co cause mild re-solution of the zinc deposit, but this occurs only after an incubation period that is dependent on the impurity concentration and on the zinc to acid ratio. Finally, a synergism often occurs among the chemical species present in the electrolyte and this complicates the prediction of impurity effects on the CE.

The effects of the elements listed in Table 1 on the electrowinning of 1-h zinc deposits from industrial acid sulphate electrolyte have been characterized in terms of deposit morphology and preferred orientation and in terms of zinc deposition current efficiency and polarization. Table 1 shows the elements studied, their atomic number and their position in the periodic table.

2. Current efficiency (CE)

The effect of the Group IIIA, IVA, VA and VIA elements listed in Table 1 on the CE for 1-h zinc deposits electrowon at 430 A m^{-2} from purified industrial acid sulphate electrolyte was determined for concentrations ranging from 0 to 50 mg l^{-1}. The effect of the Group VIII, IB and IIB elements listed in Table 1, although not part of this study, are important. Hence, the results obtained from previous work will be mentioned. The Group VIII elements, Co and Ni, had no effect on the CE for the 1-h zinc deposits for concentrations $\leqslant 5$ mg l^{-1}. For concentrations > 5 mg l^{-1} the CE decreased, particularly for Ni [1]. Other workers [2–4] have shown that an incubation period (usually

0021–891X/87 $03.00 + .12

Table 1. Partial periodic classification of the elements and their atomic numbers

VIII		*IB*	*IIB*	*IIIA*	*IVA*	*VA*	*VIA*
Co	Ni	Cu	Zn	Ga	Ge	As	Se
27	28	29	30	31	32	33	34
			Cd	In	Sn	Sb	Te
			48	49	50	51	52
				Tl	Pb	Bi	
				81	82	83	

several hours) is associated with low concentrations of Co and Ni in the electrolyte; beyond the incubation period, which is dependent on the concentration of Ni and Co in the electrolyte, the CE decreases rapidly.

Group IB (Cu) and Group IIB (Cd) elements had no effect on the CE for the 1-h zinc deposits for concentrations as high as 50 mg l^{-1} [5, 6]. The effects of Groups IIIA, IVA, VA and VIA elements on the CE for the 1-h zinc deposits (with the exception of Pb) are shown in Figs 1 and 2 as plots of CE versus impurity concentration. Fig. 1 shows the effects of Ge, Sb, Se, Te and Sn on the CE over the concentration range 0 to 2.0 mg l^{-1}. Both Ge and Sb are very detrimental to zinc deposition CE even at concentrations as low as 100 p.p.b. At 1 mg l^{-1}, both Se and Te result in a substantial decrease in the CE, to the order of 25%. Tin causes a less dramatic decrease in CE, reducing it to about 70% at 2 mg l^{-1}.

The data presented in Fig. 2 show that the effect of Sn on CE is peculiar in that as the Sn concentration increases beyond about 2 mg l^{-1}, the CE rises abruptly to about 75% and remains constant at this value for Sn concentration up to 50 mg l^{-1}. Increasing concentrations of As(V), Bi and Ga in the electrolyte result in a linear decrease in the CE for zinc deposition; the detrimental effect on the CE increased in the order As(V) > Bi > Ga. Concentrations of As(III) to 50 mg l^{-1} had no effect on the CE for the 1-h zinc deposits whereas In, Tl and Pb (not shown in Fig. 2) resulted in a slight increase in the CE.

A plot of zinc deposition current efficiency versus the atomic number of the Group IIIA to VIA elements reveals an interesting correlation (Fig. 3). The data plotted in Fig. 3 were obtained from solutions containing 10 mg l^{-1} of each element with the exception, of course, of Ge, Sb, Se and Te.

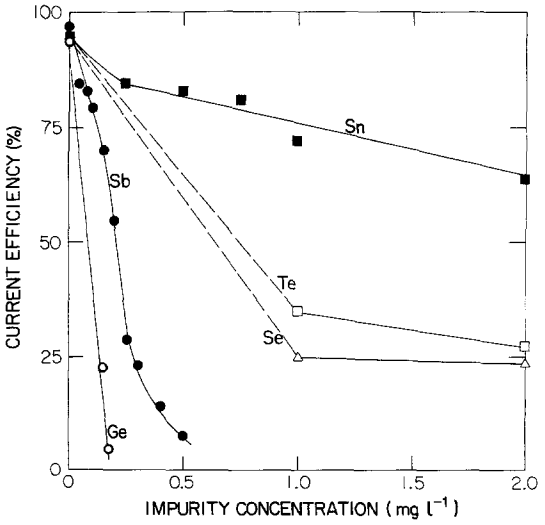

Fig. 1. The effect of increasing impurity concentration (Ge, Sb, Se, Te and Sn) on the current efficiency for 1-h zinc deposits electrowon at 430 A m^{-2} from industrial acid sulphate electrolyte.

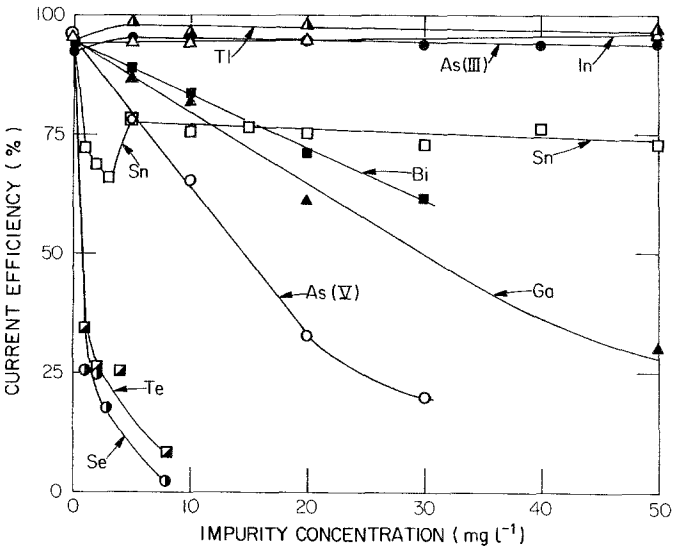

Fig. 2. The effect of increasing impurity concentration (Se, Te, Sn, As(V), Ga, Bi, As(III), In and Tl) on the current efficiency for 1-h zinc deposits electrowon at 430 A m^{-2} from industrial acid sulphate electrolyte.

For Ge and Sb the CE values obtained at 0.1 and 0.2 mg l^{-1}, respectively, were used, and for Se and Te the values obtained at 2 mg l^{-1} were employed.

The general trend is that for each period (see Table 1) the CE decreases with increasing atomic number and reaches a minimum (usually 0%) at the elements of Group VIA. In the first period illustrated Ga to Se, the decrease in CE is very sensitive to the concentration of Ge in solution and also to the oxidation state of arsenic.

The decrease in CE for zinc deposition is related to the ease with which hydrogen ions can be reduced from solution in the presence of impurities. Kita [7] showed that there was a periodic variation of the exchange current density (i_0) for the hydrogen electrode reaction with atomic number (Fig. 4). Considering the elements in Groups IIIA to VIA, the rate of hydrogen evolution increases with increasing atomic number in each period, corresponding to a similar decrease in zinc deposition CE (Fig. 3).

Two mechanisms have been proposed to explain the decrease of the CE due to the presence of impurities in the zinc electrolyte [8]. They are: (i) the reduction of H^+ on co-deposited impurities with low hydrogen overpotentials (high exchange current density) combined with localized cell corrosion, and (ii) continuous co-deposition and evolution of H_2 on zinc without preferential areas of zinc corrosion. The latter mechanism may involve interaction between the impurities and H^+ in

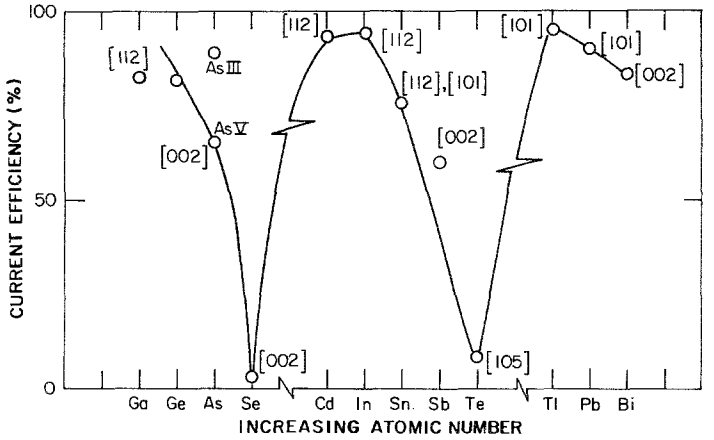

Fig. 3. Plot of zinc deposition current efficiency versus the atomic number of impurity elements.

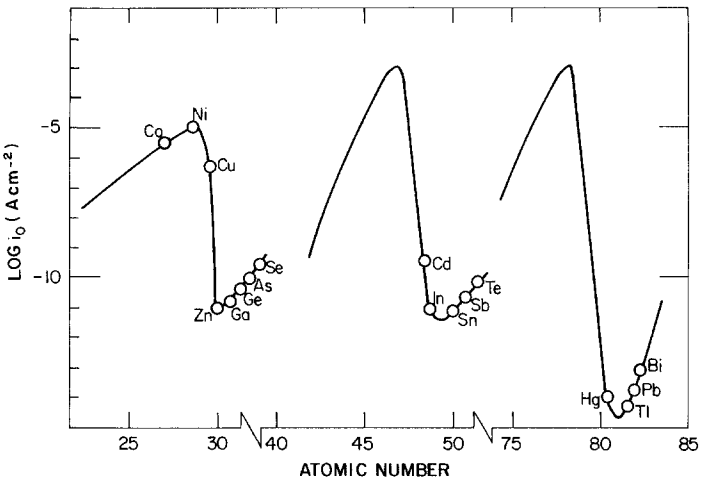

Fig. 4. Plot of the log exchange current density (i_0) of the hydrogen evolution reaction versus atomic number (after Kita [7]).

the double layer without the impurities actually depositing cathodically on zinc, e.g. the decomposition of hydrides formed in the double layer would provide an alternate path for hydrogen evolution. This theory is substantiated by the fact that the hydride-forming impurities, Ge and Sb, have never been found in the deposit, and only very small concentrations in the electrolyte are required for them to become active. Also, they have fairly high hydrogen overpotentials and would not be expected to be particularly harmful when deposited in the metallic state.

The data obtained for the co-deposition of various impurities with zinc over the 1-h electrolysis time are presented in Table 2. The deposits obtained in the presence of Ge, Sb, Se and Te were corroded severely and therefore not suitable for analysis. With the exception of Sn and Bi, those elements which co-deposited to a significant degree with zinc, i.e. Cu, Cd, Pb and Tl, either had no effect or increased the current efficiency. This is not unexpected for Cd, Pb and Tl which exhibit high hydrogen overvoltages. It may be speculated that the effect of Cu (a medium hydrogen overvoltage metal) on the CE is determined by an incubation period as for Ni and Co.

Table 2. Co-deposition of various impurities with zinc

Impurity	*Concentration in solution (mg l^{-1})*	*Concentration in zinc deposit (p.p.m.)*
Ga	50	< 80
As(III)	50	10
As(V)	10	< 6
In	50	ND
Sn	10	< 200
Sn	20	380
Sn	50	2700
Tl	50	5700
Pb	3	399
Pb	9	1535
Bi	30	2100
Cu	5	250
Cu	50	2540
Cd	5	250
Cd	50	4200

ND, not detected.
Electrolysis conditions: 55 g l^{-1} Zn; 150 g l^{-1} H_2SO_4; 35° C; 430 A m^{-2}.

Bismuth, which also has a high hydrogen overvoltage and also codeposited significantly with zinc, resulted in a substantial decrease in the current efficiency. Another high hydrogen overvoltage metal, Sn, also co-deposited extensively with Zn, particularly as its concentration in solution increased, and it also had an anomalous effect on the CE as described earlier. The different effects on the CE exhibited by the various elements that co-deposited with Zn may be related to the different deposit morphologies and orientations obtained in the presence of these elements. This is discussed in a later section.

Indium had no effect on zinc deposition CE and its presence in the zinc deposit was not detected. Both Ga and As(V), which co-deposited with zinc to a limited extent (see Table 2), had a deleterious effect on the current efficiency. Trivalent arsenic, which also co-deposited with zinc to a limited extent, had no effect on the CE for the 1-h zinc deposits.

Organic additives such as animal glue are added to the zinc electrolyte because they counteract the effect of impurities and thus maintain a high current efficiency. They also refine the deposit grain size and this results in a smooth, more compact deposit. It is often the case that there is an optimum concentration of additive, below which the CE begins to decrease. The optimum level of organic, e.g. glue, is dependent on the type and concentration of impurity. For example, the CE obtained for an electrolyte containing $0.15\,mg\,l^{-1}$ Sb is optimized at 91% when the glue concentration is $15\,mg\,l^{-1}$ (Fig. 5). For glue concentrations $< 15\,mg\,l^{-1}$, the CE decreases. A similar result is obtained for an electrolyte containing $5\,mg\,l^{-1}$ Co + $0.15\,mg\,l^{-1}$ Sb except that the decrease in CE for glue concentrations $< 15\,mg\,l^{-1}$ is more drastic (Fig. 5).

The detrimental effect of Ge on zinc electrowinning is illustrated in Fig. 6 which shows the CE obtained for 1-h zinc deposits as a function of the Ge concentration. As indicated, the CE decreases rapidly with increasing Ge concentration. For example, the CE decreased from 96 to 86% with the addition of $0.15\,mg\,l^{-1}$ Ge. At $0.3\,mg\,l^{-1}$ Ge the CE was 0%, i.e. the zinc deposit was completely redissolved. The addition of glue to the electrolyte significantly improved the CE since Ge levels in the electrolyte to $0.6\,mg\,l^{-1}$ could be tolerated before a significant decrease in CE occurred. For Ge concentrations $\leqslant 0.6\,mg\,l^{-1}$, the optimum glue concentration was $15\,mg\,l^{-1}$. At higher Ge concentrations, e.g. $1\,mg\,l^{-1}$, the CE decreased to $< 55\%$ even in the presence of $30\,mg\,l^{-1}$ glue.

Fig. 7 shows the effect of increasing glue concentration on the CE for electrolytes containing a fixed concentration of various impurities. The beneficial effect of glue on the CE for electrolytes containing $0.135\,mg\,l^{-1}$ Ge and $0.20\,mg\,l^{-1}$ Sb is clearly indicated. The situation with respect to glue–Sn interaction is somewhat anomalous. For an electrolyte containing $1\,mg\,l^{-1}$ Sn, increasing glue additions at first result in a decrease in CE (Fig. 7). The CE reaches a minimum at $15\,mg\,l^{-1}$ glue and then begins to increase, reaching a maximum value at about $40\,mg\,l^{-1}$ glue.

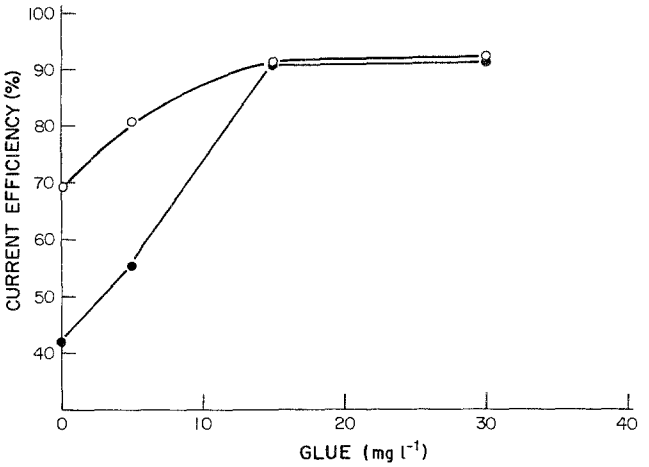

Fig. 5. Plots showing the effect of increasing glue concentration in combination with antimony and cobalt on the current efficiency for 1-h zinc deposits electrowon at $430\,A\,m^{-2}$ from industrial acid sulphate electrolyte. (○) No Co, $0.15\,mg\,l^{-1}$ Sb; (●) $5\,mg\,l^{-1}$ Co, $0.15\,mg\,l^{-1}$ Sb.

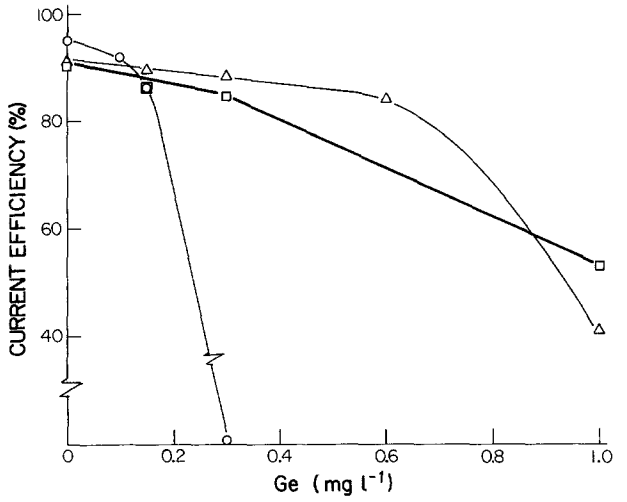

Fig. 6. Plots showing the effect of increasing germanium concentration in the presence and absence of glue on the current efficiency for 1-h zinc deposits electrowon from industrial acid sulphate electrolyte. (○) Ge only; (△) Ge + 15 mg l^{-1} glue; (□) Ge + 30 mg l^{-1} glue.

Increasing glue concentration in an electrolyte containing no added impurities results in a slight decrease in the CE. This is also the case for electrolytes containing As(III), Tl, Ga, Bi and Te. According to the results presented in Fig. 7, glue has a negative interaction with As(V) and Se, i.e. the CE decreases with increasing glue concentration.

3. Deposit morphology and orientation

The presence of the various elements listed in Table 1 in the purified acid sulphate electrolyte resulted in 1-h zinc deposits consisting of four distinct morphology types (Fig. 8). These morphology types had certain preferred zinc deposit orientations defined by the angle at which the basal plane was aligned to the aluminium cathode (Table 3).

The intermediate morphology, Fig. 8a, consisted of well-defined hexagonal zinc platelets aligned at angles of 30–70° to the Al cathode and exhibited a (1 1 4), (1 1 2), (1 0 2) preferred orientation (Table 3). This morphology type was usually associated with high current efficiency, and was obtained from addition-free electrolyte and from electrolytes containing Co, Ni, Cu, Ga, Ge,

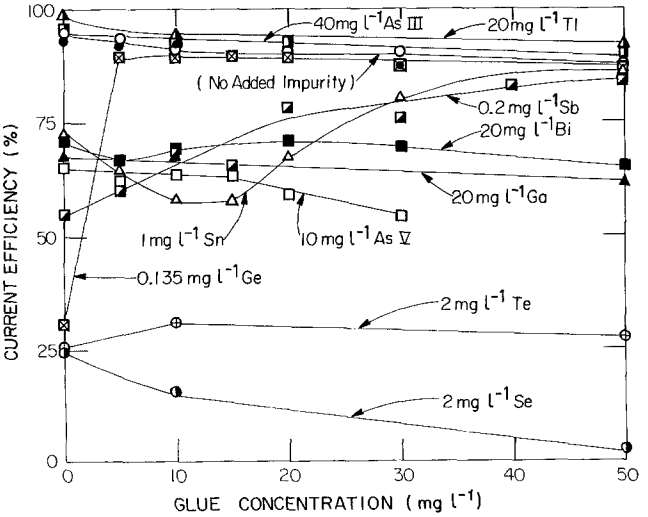

Fig. 7. The effect of increasing glue concentration alone and in the presence of a fixed concentration of the various impurities on the current efficiency for 1-h zinc deposits electrowon at 430 A m^{-2} from industrial acid sulphate electrolyte.

Table 3. Zinc deposit morphologies with corresponding orientations

Morphology type	*Platelet alignment to aluminium substrate*	*Preferred orientation*[a]
Basal	0–30°	[0 0 2], [1 0 3], [1 0 5]
Intermediate	30–70°	[1 1 4], [1 1 2], [1 0 2]
Triangular	70°	[1 0 1]
Vertical	70–90°	[1 0 0], [1 1 0]

[a] Relative to ASTM standard for zinc dust.

As(III), Cd and In. The elements Co, Ni, Cu and Cd affected the morphology in that they reduced the size of the zinc platelets relative to the addition-free electrolyte. As(III) and In had no effect on the platelet size. Although producing this morphology type, both Ga and Ge substantially reduced the CE for the 1-h zinc deposits perhaps indicating a different mechanism for hydrogen evolution in the presence of these impurities.

Another morphology type (Fig. 8b) very close to intermediate, has been termed triangular. It consists of hexagonal platelets aligned at high angles ($\sim 70°$) to the Al surface and has a predominant (1 0 1) preferred orientation. This morphology type has been found only in the presence of Pb and Tl and for low concentrations of glue. It also is associated with high CE for zinc deposition. A variation of this morphology type has been observed for low concentrations of Pb and Tl ($< 3\,mg\,l^{-1}$) and is shown in Fig. 8c. In this case the preferred orientation remains (1 0 1) but the zinc platelets are increased in size and often have serrated edges.

The vertical morphology type, Fig. 8d, is commonly associated with solutions containing high glue concentrations ($> 30\,mg\,l^{-1}$) or solutions containing Pb and glue. The zinc platelets are aligned at $\sim 90°$ to the Al surface and the preferred orientation is (1 0 0), (1 1 0). The current efficiency is normally high for this morphology type.

The basal morphology type is exemplified by the SEM photomicrographs shown in Fig. 8e and 8f. This morphology is characterized by hexagonal zinc platelets oriented at low angles to the Al substrate (0–30°); the platelets are either large, flat and well-defined (Fig. 8e) or they are arranged

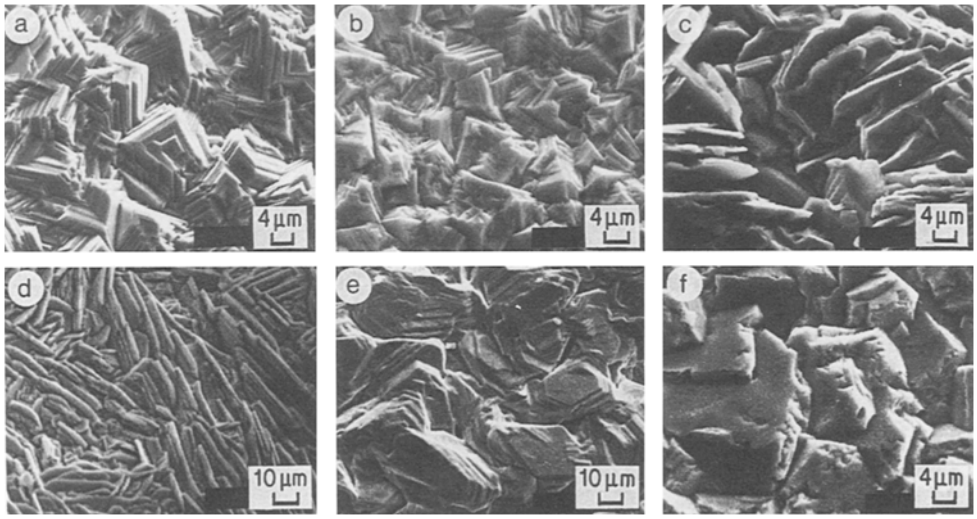

Fig. 8. SEM photomicrographs showing the four main characteristic zinc deposit morphologies: (a) Intermediate; (b) triangular, type 1; (c) triangular, type 2; (d) vertical; (e) basal, type 1; (f) basal, type 2.

Table 4. The effect of impurities and their interaction with glue on the preferred orientation of zinc deposits electrowon from industrial acid sulphate electrolyte

Impurity	*Concentration* ($mg\,l^{-1}$)	*Glue* ($mg\,l^{-1}$)	*Orientation*
None added	0	0	(1 1 2) (1 1 4) (1 0 2)
	0	30	(1 0 1)
Ga	20	0	(1 1 2)
	20	10	(1 1 2)
	20	50	(1 0 1)
In	20	0	(1 1 2) (1 0 3)
	20	20	(1 1 4) (1 0 1)
Tl	20	0	(1 0 1)
	20	10	(1 0 0) (1 1 0) (1 1 2)
Ge	0.15	0	(1 1 2) (1 1 0)
	0.15	30	(1 1 2) (1 1 0)
Sn	1.0	0	(1 0 3)
	1.0	30	(1 0 5)
	1.0	50	(0 0 2)
Pb	3	0	(1 0 1)
	3	30	(1 1 2) (1 0 1)
As(III)	50	0	(1 1 2)
	40	20	(1 0 1)
As(V)	10	0	(1 1 4) (1 1 2)
	10	10	(1 0 1)
	10	10	(1 0 1)
Sb	0.04	0	(1 0 3) (0 0 2)
	0.04	20	(1 1 2) (1 1 4) (1 0 2)
Bi	20	0	(0 0 2)
	20	50	(0 0 2)
Se	2	0	(0 0 2)
	2	10	(0 0 2)
Te	2	0	(1 0 5)
	2	10	(1 0 1) (1 0 0)

in non-distinct clusters of irregularly shaped crystals (Fig. 8f). The preferred orientation is (0 0 2), (1 0 3), (1 0 5) and the CE is usually very low. This morphology type is typical of the elements Sb, Se, Te, As(V), Bi and low concentrations of Sn. This morphology type seems to facilitate hydrogen evolution and may be the reason why Bi causes a large decrease in CE whereas Pb and Tl do not.

The interaction of glue with the various impurities also can result in changes in the deposit morphology and orientation. Although only the four morphology types listed in Table 3 result, certain combinations of glue and impurity can cause a change from one morphology type to another. A good example of this is the interaction between glue and Sb. As mentioned above, the presence of glue in the zinc electrolyte results in a triangular-type morphology, (1 0 1) preferred orientation (Fig. 8b), whereas Sb-containing electrolytes result in a basal-type morphology, i.e. large, flat platelets, (0 0 2) preferred orientation (Fig. 8e). Certain combinations of glue + Sb, e.g. $15\,mg\,l^{-1}$ glue + $0.04\,mg\,l^{-1}$ Sb or $30\,mg\,l^{-1}$ glue + $0.08\,mg\,l^{-1}$ Sb, produce an intermediate-type morphology, (1 1 2) (1 1 4) (1 0 2) preferred orientation (Fig. 8a), identical to that obtained from addition-free electrolyte (Table 4).

The effect of various impurities including antimony and their interaction with glue on the preferred orientation of zinc deposits electrowon from industrial acid sulphate electrolyte are summarized in Table 4. As noted earlier, glue has a positive effect in improving the CE in the presence of Sb, Ge, Sn and Te. For the remaining impurities listed in Table 4, glue either had no effect or caused a further decrease in CE. By the same token, glue changed the preferred orientation obtained for Sb from (1 0 3) (0 0 2) to (1 1 2) (1 1 4) (1 0 2) and for Te from (1 0 5) to (1 0 1) (1 0 0). Although the presence of glue increased the CE for Ge-containing electrolyte, the preferred orientation did not change. As mentioned earlier, the glue–Sn interaction is anomalous. Although increased glue additions (i.e. 50 mg l^{-1}) increased the CE for electrolytes containing 1 mg l^{-1} Sn, the orientation became more basal and changed from (1 0 5) to (0 0 2). In other instances the addition of glue to solutions containing impurities such as Ga, In, As(III) and As(V) resulted in a glue-type orientation, i.e. (1 0 1). The interaction between glue and Bi and glue and Se is negative, i.e. the CE decreases and the deposit orientation remains (0 0 2) (Table 4).

4. Zinc deposition polarization

Cyclic voltammetry is a convenient technique for measuring zinc deposition polarization effects. A typical voltammogram obtained for zinc deposition from an addition-free electrolyte is shown in Fig. 9. A cycle starting from point A (−0.85 V vs SCE) goes through a region of low current until point C where zinc deposition commences. The current increases to point D where the scan is reversed. The current then decreases and reaches zero at point B where it becomes anodic corresponding to the dissolution of deposited zinc. The anodic peak is reached at E and dissolution is complete on return to A.

The region CDB is called a nucleation hysteresis loop and is characterized by several important features. The current for the initial deposition of zinc (point C) does not become appreciable until well beyond the reversible zinc potential. The point C has been used to define a 'nucleation overpotential' CB. As noted by Biegler [9], however, the position of C can be defined only loosely as it appears to shift with the sensitivity at which the current is recorded and with the sweep rate. The position of C also shifts when certain impurities and/or organics are added to the electrolyte.

The current on the descending branch of the loop (DB) is higher than on the ascending branch because, at a given potential, there are more and larger zinc nuclei available but the charge transfer rate constant is the same. The cathodic overpotential in this region is associated mostly with zinc deposition onto freshly deposited zinc and has been termed the 'plating overpotential' [10]. The plating overpotential has been found to be sensitive to the presence of certain organic additives in

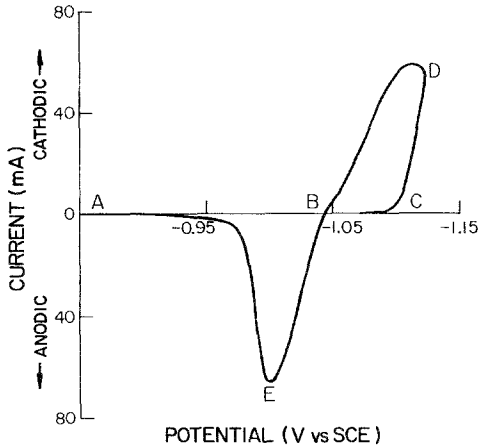

Fig. 9. Cyclic voltammogram obtained for addition-free industrial acid zinc sulphate electrolyte. Sweep rate, 2 mV s^{-1}.

both lead and copper electrorefining. The descending branch crosses the zero current axis at point B, the crossover potential, at or close to the reversible potential of the system.

The cyclic voltammogram for zinc deposition is very sensitive to the impurities present in the electrolyte. The nucleation overpotential (NOP) (section C-B in Fig. 9) is sensitive to some impurities but not others. For example, Sb decreases the NOP whereas Pb and Tl increase it. Impurities such as In, Cd, As(III), Cu, Co and Ni have no effect on the NOP. The reverse scan portion of the cyclic voltammogram, DB, termed the plating overpotential (POP) and the crossover potential (point B of Fig. 9), are quite sensitive to other impurities such as As(V), Sn, Ge, Ga, Se and Te. As(III), like In and Cd, has no effect on these segments of the cyclic voltammogram, but unlike In and Cd, As(III) produces a characteristic Pre-wave prior to zinc deposition.

An example of the effect of certain impurities and additives, such as glue, on the NOP is shown in Fig. 10. In this figure only the BDC portions of the cyclic voltammograms are shown to illustrate the effect of Sb and glue, alone and in combination, on zinc deposition polarization. Curve a of Fig. 10 represents zinc deposition from addition-free purified zinc electrolyte. Curve b was obtained by adding $0.08\,mg\,l^{-1}$ Sb to the purified electrolyte; relative to curve a, the addition of Sb has depolarized (decreased the NOP) zinc deposition. The addition of $10\,mg\,l^{-1}$ glue to the purified electrolyte results in a significant increase in NOP (compare curves c and a). The combined addition of $0.08\,mg\,l^{-1}$ Sb and $10\,mg\,l^{-1}$ glue resulted in polarization curve d, which lies very close to curve a, the addition-free trace.

The effects of Sb and glue on the NOP for zinc deposition suggest a correlation between the observed zinc deposit morphology (and orientation) and deposition overvoltage. The morphology obtained with impurities, such as Sb, which depolarize zinc deposition (decrease NOP) is characterized by large crystal facets aligned at low angles to the Al cathode (see Fig. 8d and 8e). The resulting deposit exhibits a preferred (0 0 2) (1 0 3) (1 0 5) orientation (Table 3). Since there is always some co-deposition of H^+ with zinc it is likely that H^+ adsorption has an effect on zinc deposition polarization. Antimony can depolarize the reaction by interfering with the adsorption of H^+ by forming volatile hydrides and thus provide an alternate path for hydrogen evolution. The fact that depolarization causes a decrease in zinc nucleation accounts for the increase in zinc platelet size observed when Sb is present in the electrolyte.

The zinc deposit morphology obtained when glue is added to the electrolyte (Fig. 8b) is characterized by a strong preference for (1 0 1) orientation. The substantial increase in the NOP (Fig. 10) observed for glue additions may result from the zinc having to deposit through a glue adsorption layer, and the preferred (1 0 1) orientation may result from the glue increasing the overpotential preferentially on selected planes. The increased polarization observed in the presence of glue leads to increased nucleation, and this results in a substantial decrease in zinc platelet size.

The combined addition of Sb + glue resulted in an NOP (Fig. 10, curve d) and a deposit morphology (Fig. 8a) very similar to those obtained for the addition-free electrolyte. This suggests that the opposing influences of Sb and glue on the NOP tend to counteract each other, resulting in an overpotential which is indicative of the preferred morphology. The proper combinations of Sb and glue which give rise to the preferred deposit morphology also optimize the CE for zinc

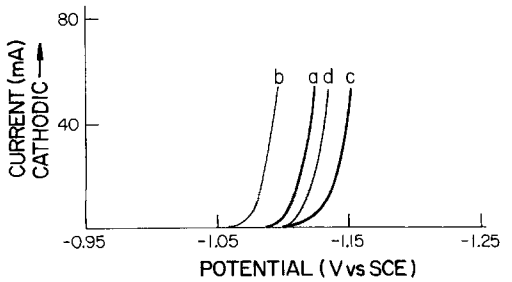

Fig. 10. Current versus potential plots showing the effect of antimony and glue on the CD portion of the zinc deposition cyclic voltammogram. Sweep rate, $2\,mV\,s^{-1}$. (a) No addition; (b) $0.08\,mg\,l^{-1}$ Sb; (c) $10\,mg\,l^{-1}$ glue; (d) $0.08\,mg\,l^{-1}$ Sb + $10\,mg\,l^{-1}$ glue.

deposition as shown earlier. The relationships between zinc deposit preferred orientation, electrolyte additions such as Sb and glue, the CE and the overpotentials associated with zinc deposition can be summarized as follows:

Excess Sb		Addition-free or Sb + glue		Excess glue
(0 0 2) ←	(1 0 5) (1 0 3) ←	(1 1 2) (1 1 4) (1 0 2)	→ (1 0 1) →	(1 0 1) (1 0 0)
decreasing ←		overpotential		→ increasing
decreasing ←		CE optimum		→ decreasing

Although Sb and glue have a pronounced effect on the NOP for zinc deposition, impurities such as Ge, Co and Ni, which can be as harmful as Sb, do not cause a significant change in the ACD forward scan portion of the cyclic voltammogram (Fig. 9). Certain impurities, however, including Ge, Co and Ni, result in characteristic changes in the voltammograms which appear during the reverse scan, i.e. after the potential has been reversed. Certain impurities such as Ge and As(V) result in a significant change in the DB portion of the voltammogram (Fig. 9), i.e. they appear to affect the POP for zinc deposition. In addition, the BEA portion of the voltammogram, i.e. the anodic dissolution of zinc, is considerably reduced in the presence of these impurities.

The voltammograms obtained for zinc deposition from electrolytes containing 0.64 and 0.96 mg l^{-1} Ge are compared to that for a Ge-free electrolyte in Fig. 11. At 0.64 mg l^{-1} Ge, a shoulder appears in the DB portion of the voltammogram prior to the zero current or crossover potential, B. The potential B is also shifted to a more positive value and the anodic portion of the voltammogram, BEA, is substantially reduced. At 0.96 mg l^{-1} Ge, the shoulder is more pronounced and occurs earlier in the reverse scan; the crossover potential (B) is even more positive and the anodic portion of the voltammogram is much smaller than that for a Ge concentration of 0.64 mg l^{-1}. The value of the cathodic current associated with the shoulders of the voltammograms for Ge-containing electrolytes (Fig. 11) increases linearly with increasing Ge concentration. Vigorous H_2 evolution is observed at the cathode surface when the potential is in the region of the shoulder on the voltammogram.

In Fig. 12 the voltammogram obtained for zinc deposition from electrolyte containing 0.3 and 10 mg l^{-1} Ni are compared. These voltammograms are different from those obtained for Ge-containing electrolyte (cf. Fig. 11). The cathodic portions of the voltammograms CDB (Fig. 12) are similar. In the presence of Ni, however, there is a substantial reduction in the anodic portion of the

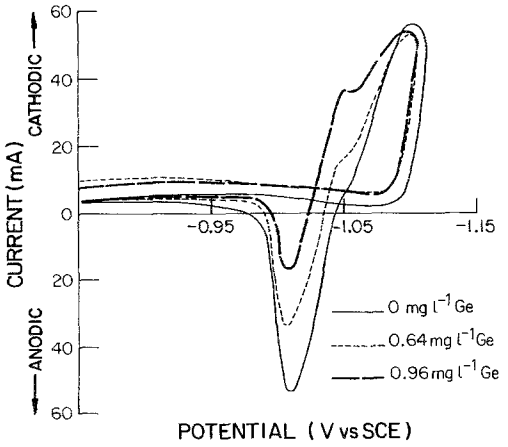

Fig. 11. Cyclic voltammograms showing the effect of germanium on zinc deposition polarization. Sweep rate, 2 mV s^{-1}.

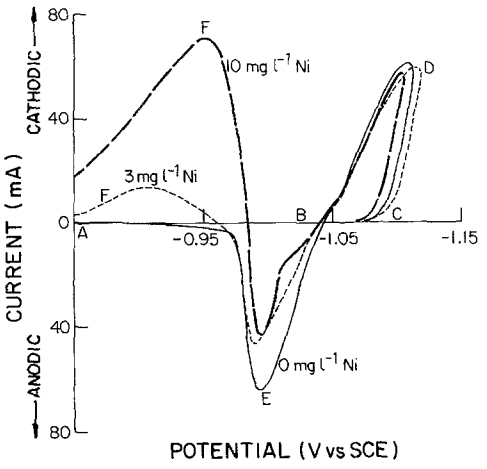

Fig. 12. Cyclic voltammograms showing the effect of nickel on zinc deposition polarization. Sweep rate, $2\,mV\,s^{-1}$.

curve (BEA), indicating that some zinc re-solution may have occurred prior to the cathodic current reaching its zero value at point B. This behaviour may be the result of H_2 evolution on co-deposited Ni being the cathodic reaction and zinc dissolution being the corresponding anodic reaction. In addition, there is a substantial cathodic current after the zinc has been anodically stripped from the surface point F on Fig. 12. This is probably due to H^+ ion reduction. Vigorous H_2 evolution is observed at this point, and this indicates that some Ni must remain on the surface of the Al cathode. The cathodic current at F increases linearly with increasing Ni concentration in the electrolyte. Thus, the characteristic features of the voltammograms in Figs 11 and 12 might be useful as a rapid means for detecting the presence of Ge and Ni, respectively, in zinc electrolyte.

It is possible that impurities can exist in different oxidation states in the zinc electrolyte and hence produce different electrochemical effects on zinc deposition. O'Keefe [11] compared the polarization behaviour of Sb(III) and Sb(V) using neutral and slightly acidic ($5\,g\,l^{-1}$ H_2SO_4) zinc sulphate electrolytes. He reported that both forms of Sb caused depolarization of zinc deposition, but that Sb(III) seemed to be more potent than Sb(V) in acid solution. Sb(V) increased polarization as the pH decreased.

Cyclic voltammograms obtained from electrolytes containing $50\,mg\,l^{-1}$ As(III) and $9\,mg\,l^{-1}$ As(V) are compared to that obtained from an arsenic-free electrolyte in Fig. 13. The presence of $50\,mg\,l^{-1}$ As(III) in the electrolyte results in a significant cathodic current prior to the zinc decomposition potential; however, the remainder of the voltammogram is similar to the arsenic-free curve, except that the current again becomes cathodic following the anodic dissolution of deposited zinc.

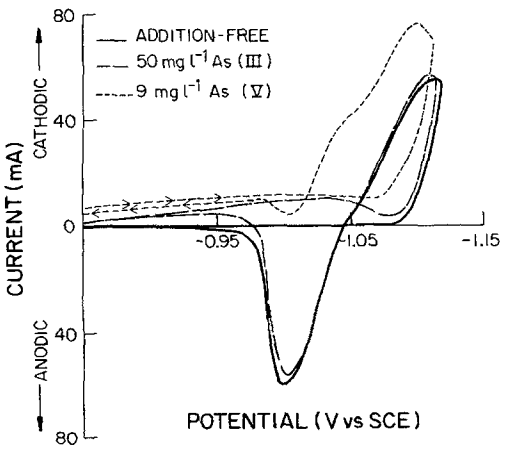

Fig. 13. Cyclic voltammograms showing the effects of As(III) and As(V) on zinc deposition polarization. Sweep rate, $2\,mV\,s^{-1}$.

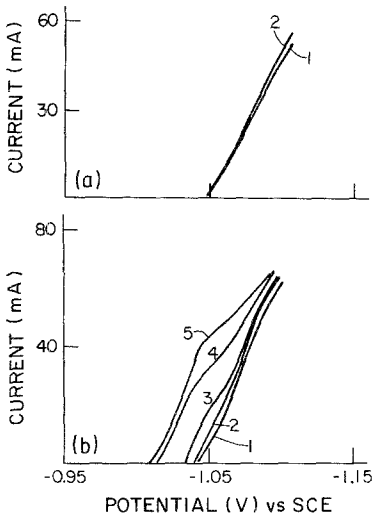

Fig. 14. The 'DB' portions of the cyclic voltammograms showing the effect of (a) As(III) concentration and (b) As(V) concentration on the plating overpotential for zinc deposition. (a) As(III) concentration ($mg\,l^{-1}$): curve 1, 0; curve 2, 50. (b) As(IV) concentration ($mg\,l^{-1}$): curve 1, 0; curve 2, 1; curve 3, 6; curve 4, 9; curve 5, 12.

The initial stage of the voltammogram obtained in the presence of $9\,mg\,l^{-1}$ As(V) is similar to that for As(III). As(V), however, causes a significant decrease in the zinc decomposition potential, i.e. in the NOP. Also, the reverse scan is characterized by a plateau region similar to that observed for Ge (Fig. 11). In the case of As(V) there is no anodic current, and this indicates that all the previously deposited zinc dissolved when the current was cathodic. Thus, during the reverse scan the plateau region and beyond is probably due to H_2 evolution (vigorous gassing occurs in this region) with concomitant zinc dissolution as the corresponding anodic half-reaction.

The main difference between the As(III) and As(V) voltammograms is shown more clearly in Fig. 14 in which only the reverse cathodic portions (DB) are shown as a function of increasing As(III) and As(V) concentrations. As indicated in Fig. 14a, increasing the As(III) concentration to $50\,mg\,l^{-1}$ has no significant effect on the 'DB' portion of the voltammogram, i.e. on the zinc POP. Increasing the As(V) concentration (Fig. 14b), on the other hand, has a significant effect on both

Table 5. Effect of various impurities on the characteristic features of the zinc deposition cyclic voltammogram

Impurity	*Pre-wave*	*Nucleation overpotential (NOP)*[a]	*Plating overpotential (POP)*[a]	*Crossover potential*[a]
In	no	no	no	no
Cd	no	no	no	no
As(III)	yes	no	no	no
Pb	no	increase	increase	no
Tl	no	increase	increase	no
Co	no	no	decrease	decrease
Ni	no	no	decrease	decrease
Cu	yes	no	increase	increase
As(V)	yes	decrease	decrease	decrease
Sb	no	decrease	no	no
Sn	no	decrease	decrease	no
Ge	no	decrease	decrease	decrease
Ga	yes	decrease	decrease	decrease
Bi	no	decrease	no	slight decrease
Se	no	decrease	decrease	decrease
Te	no	decrease	decrease	decrease

[a] Relative to addition-free electrolyte.
Experimental conditions: $55\,g\,l^{-1}$ Zn; $150\,g\,l^{-1}$ H_2SO_4; 25°C; $2\,mV\,s^{-1}$; -0.95 to -1.15 V vs SCE.

the shape and position of the 'DB' curves relative to an electrolyte containing no added As(V). Thus, it appears that the POP for zinc deposition is sensitive to As(V) but not to As(III).

These results indicate that polarization techniques appear promising as an analytical test to determine the quality of zinc sulphate electrolyte prior to electrolysis. The effects of the various impurities, relative to the addition-free electrolyte, on the characteristic features of the zinc deposition cyclic voltammogram are summarized in Table 5.

In Table 5 the effects of the various impurities on the cyclic voltammogram for zinc deposition are considered under four main categories, namely (i) whether or not the impurity results in a 'prewave' prior to zinc deposition, (ii) whether or not the impurity results in an increase or decrease in the NOP, (iii) whether or not there is an increase or decrease in the POP, and (iv) whether or not there is an effect on the crossover potential. As indicated in Table 5, only four of the impurities studied, i.e. As(III), Cu, As(V) and Ga show a pre-wave in the cyclic voltammogram. As(V) and Ga produce similar effects on the NOP, POP and crossover potential. As(III) and Cu produce different effects on the NOP, POP and crossover potential both with respect to As(V) and Ga, as well as to each other. Thus, by comparing voltammograms it may be possible to identify a specific impurity in the zinc electrolyte.

5. Conclusions

The effects of 15 elements and their interaction with glue on zinc electrowinning from industrial acid sulphate electrolyte have been characterized in terms of deposit morphology and orientation and in terms of zinc deposition current efficiency and polarization behaviour. Both As(III) and As(V) were studied.

It was observed that the zinc deposition CE decreased with increasing atomic number of the elements in each period of the periodic table. The decrease in CE paralleled a corresponding increase in the rate of hydrogen evolution which increased with increasing atomic number in each period. The elements most detrimental to zinc deposition were Ge, Sb, Se and Te followed by Sn, As(V), Bi and Ga. As(III) had no effect on the CE of zinc deposition whereas In, Pb and Tl resulted in a slight increase in CE.

The addition of glue to the electrolyte counteracted the detrimental effects of Sb and Ge on the CE of zinc deposition. Glue had virtually no effect on the CE for zinc deposition from electrolytes containing As(III), Tl, Ga, Bi and Te. Glue, however, had a negative interaction with As(V) and Se, i.e. the CE decreased with increasing glue concentration. The glue–Sn interaction was anomalous in that the CE decreased, reached a minimum, and then increased with increasing glue concentration.

The presence of these elements in the electrolyte also affected the zinc deposit morphology and orientation. Four distinct morphology types with corresponding orientations were observed. Addition-free electrolyte (i.e. containing no added impurities or added glue) and electrolytes containing Co, Ni, Cu, Ga, Ge, As(III), Cd and In resulted in an intermediate-type morphology consisting of well-defined zinc platelets aligned at 30–70° angles to the Al cathode. The preferred orientation was [1 1 4] [1 1 2] [1 0 2]. The presence of Tl, Pb or low concentrations of glue produced a triangular-type morphology in which the platelets were aligned at high angles $\sim 70°$ to the Al cathode. The preferred orientation was [1 0 1]. A vertical-type morphology, platelets aligned at $\sim 90°$ to the Al surface, resulted when the electrolyte contained high glue concentrations or contained both Pb and glue. The preferred orientation was [1 0 0] [1 1 0]. The basal morphology type, characterized by zinc platelets oriented at low angles ($\leqslant 30°$) to the Al cathode, resulted when the electrolyte contained Sb, Se, Te, As(V), Sn and Bi. The preferred orientation was [0 0 2] [1 0 3] [1 0 5].

The impurities also affected the zinc deposition cyclic voltammograms. Certain impurities such as Sb, Pb and Tl affected the nucleation overpotential whereas others such as As(V), Sn, Ge and Ga affected the plating overpotential. Trivalent arsenic resulted in a characteristic pre-wave prior to zinc

deposition whereas Ni and Co produced a significant cathodic current in the reverse scan following zinc stripping. Thus, polarization measurements such as cyclic voltammetry are promising as a diagnostic test to determine the quality of zinc sulphate electrolyte prior to electrolysis. By comparing voltammograms it may be possible to identify specific impurities in the zinc electrolyte.

Acknowledgements

Thanks are due to Cominco Ltd for providing the electrolyte. D. Owens, CANMET, performed the scanning electron microscopy of the zinc deposits, and P. Carriere, CANMET, carried out the X-ray diffraction analyses.

References

[1] D. J. MacKinnon, J. M. Brannen and R. M. Morrison, *J. Appl. Electrochem.* **16** (1986) 53.
[2] M. Maja and P. Spinelli, *J. Electrochem. Soc.* **118** (1971) 1538.
[3] M. Maja, N. Penazzi, R. Fratesi and G. Roventi, *ibid.* **129** (1982) 2695.
[4] I. W. Wark, *J. Appl. Electrochem.* **9** (1979) 721.
[5] D. J. MacKinnon, *ibid.* **15** (1985) 953.
[6] D. J. MacKinnon, J. M. Brannen and R. C. Kerby, *ibid.* **9** (1979) 71.
[7] H. Kita, *J. Electrochem. Soc.* **113** (1966) 1095.
[8] H. Fukubayashi, T. J. O'Keefe and W. C. Clinton, 'Effects of the Impurities and Additives on the Electrowinning of Zinc', US Bureau of Mines Report of Investigations, RI 7966 (1974) p. 26.
[9] T. Biegler, in 'The Application of Polarization Measurements in the Control of Metal Deposition' (edited by I. H. Warren), Elsevier Publishing Co. (1984) p. 32.
[10] T. N. Andersen, R. C. Kerby and T. J. O'Keefe, *J. Metals* **37** (1985) 36.
[11] T. J. O'Keefe, *J. Electroanal. Chem.* **168** (1984) 131.